A SPARK GAP MODEL FOR LTSPICE AND SIMILAR CIRCUIT SIMULATION SOFTWARE

J. Cameron Pouncey, Jane M. Lehr
University of New Mexico, MSC 01 110, 1 University of New Mexico
Albuquerque, NM 87131 USA

Abstract

In the past, the simulation of pulsed power circuits used specifically designed programs such as Sandia's SCREAMER, NRL's BERTHA, or the industry developed TL Code. These codes incorporated specialized models for many pulsed power components which captured key manifestations of the physical phenomena. Now, the simulation of pulsed power circuits is likely to be accomplished with the ubiquitous SPICE-based software. Of the available software, LTspice, a program developed by semiconductor manufacturer Linear Technology Corp, has become very prevalent due to its ease of use, continuous improvement, and free availability. However, LTspice - like all SPICE programs - does not include realistic models for key pulsed power circuit devices – including the spark gap switch. While simple switch models do exist in LTspice and other SPICE programs, these can only crudely approximate the behavior of a spark gap. This effort focuses on developing an LTspice circuit model for a gas-filled spark gap switch that is physically realistic while being simple enough as to permit simulations to run in reasonable times on typical personal computers. Efforts are made to create a model that is portable between different SPICE programs with minimal modification.

I. INTRODUCTION

Lumped element circuit simulation software using the SPICE algorithm has been used for some time in the modeling of pulsed power systems. Elements like capacitors, inductors, and even transmission lines can be easily incorporated into simulations via models native to the SPICE environment. Spark gap switches, however, are not native components of the software and thus must be approximated by some combination of other circuit elements.

Two very different difficulties are encountered when modeling a spark gap in SPICE. The first is the computational convergence of the simulation solution caused by the abrupt change in the impedance of the spark gap and its compatibility with the SPICE algorithm. SPICE software generally allows for the simulation tolerances to be adjusted, helping the simulation converge. The second has to do with the accuracy of the spark gap model itself. For instance, the impedance of a spark gap does not change linearly from its high impedance "open" state to its low impedance "closed state" – that change occurs as some function of gap current, time, and other parameters.

While previous investigators have reported various SPICE spark gap models for specific applications [1]–[4], we believe that the approach presented here will provide practitioners in the pulsed power field with a tool of broad applicability and useful predictive capabilities. The available scaling expressions for key physical phenomena have been brought together and implemented in LT-SPICE with the intent to provide a physics-based model which accurately predicts the behavior of an air insulated spark gap. In the proposed spark gap model, the inputs to the code are the gas pressure, gap capacitance, and the gap length.

II. MODEL DESCRIPTION

A. Assumptions

While it has been the goal to make the model described in this paper as generally applicable as possible, certain assumptions have been made in order to provide some bounds to the scope of the problem. First, it has been assumed that this model will be used to simulate gas spark gaps with gas pressure and electrode spacing that put operation well to the right of the Paschen minimum. It has also been assumed that the model will be used to simulate spark gaps used as switches where the external circuit will be capable of providing the current necessary to ensure the transition to a true arc mode of operation. It has also been assumed that the user will provide certain input parameters for the model. In particular, the gap separation distance, gas pressure, and stray capacitance are the minimum input parameters for the model as presented.

B. Notation

In this paper, the following notation will be used when referring to the components, parameters, and values of the model. Circuit device names will be identified by bold-face type – e.g. **S_Ch**. Node names will be given in italic font – e.g. *Ch_On*. The voltage at a node will be designated as V(<node name>), likewise the current through a device as I(<device name>) – e.g. V(Ch_on) or I(S_Ch). The names of model parameters will be written enclosed in curly braces, except when they are used in equations – e.g {Ron} and Ron+1.

978-1-4799-8403-9/15/$31.00 ©2015 IEEE

C. Framework

The model described in this paper is based on a framework that is intended to provide a means of implementing all of the relevant physics of a spark gap switch in a way that can be tailored to the requirements of a particular user. The basic circuit of the spark gap, as shown in Figure 1, consists of only two terminals and four elements. The terminals are the nodes *T1* and *T2*. They provide the points of interconnection for this model when it is used as a subcircuit in a user simulation. In a physical sense, these points represent the face of each electrode of the spark gap. Any parasitic components of the physical switch under investigation must be added external to this model. The first element is a behavioral current source, **B_Ind**, which is used to model the parametric inductance of the channel. This is followed by the voltage controlled switch, **S_Ch**, which models the transition that occurs when a channel initially forms across the entire gap. In series with this switch is the behavioral voltage source, **B_Res**, which is used to model the parametric resistance of the channel. In parallel with the series combination of these three components is **C_Gap**, which represents the fixed capacitance between the gap electrodes and is parameterized by the user input parameter {C}.

Separate from this main circuit are the various behavioral sources and associated circuitry that provide the means of calculating the various parameters that are used to control the behavior of the main circuit elements. The behavioral sources are used to generate voltages that represent actual physical quantities of the spark gap during operation. These voltages are available at descriptively named nodes. The equations that control each of the behavioral sources can be modified by the user as necessary to implement a preferred model of the physical process.

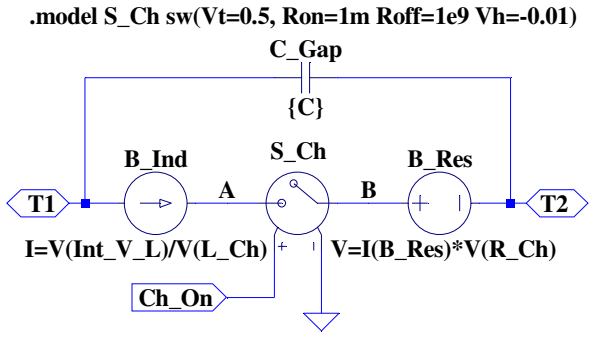

Figure 1. Main Spark Gap Circuit

D. Breakdown Modeling

The accurate modeling of the breakdown of the gap under the influence of the applied voltage is very important for the accuracy and applicability of the model. Thus, effort has been made to capture all of the various parameters and processes which influence breakdown and incorporate them in the modular framework of this model. The various processes that could influence breakdown are modeled by the circuitry shown in Figure 2.

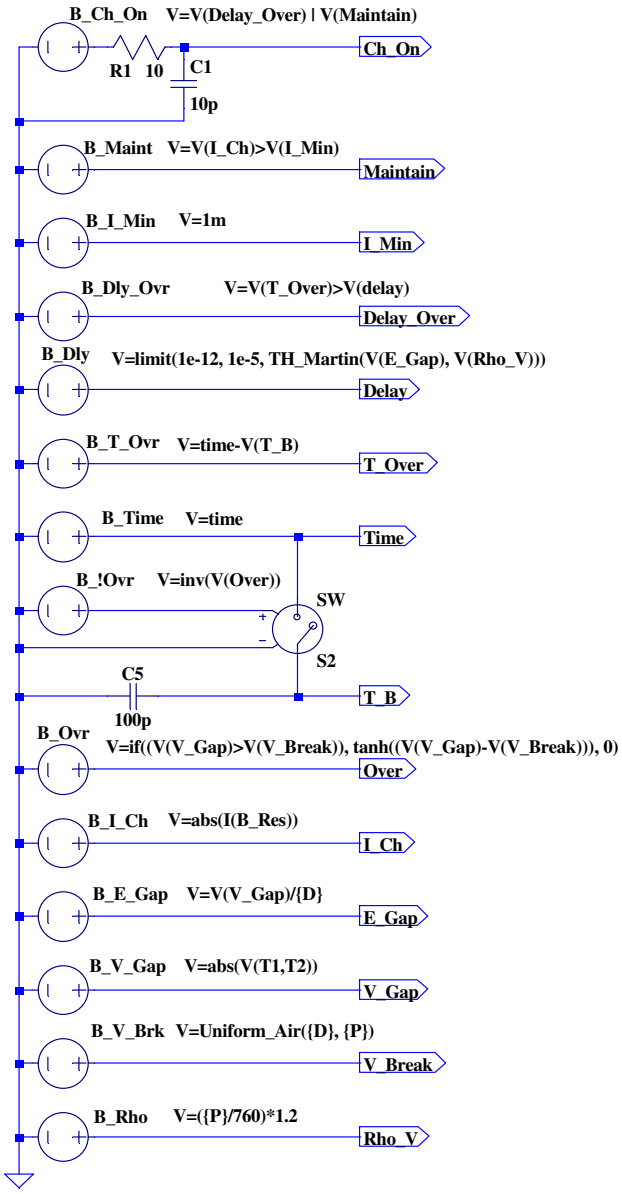

Figure 2. Breakdown Control Circuitry

1) Control of Channel Closure

In the present model, breakdown is defined as the transition of switch **S_Ch** from the off to the on state. The model statement for **S_Ch** is defined with the parameters for off-state resistance {Roff}, on-state resistance {Ron}, threshold voltage {Vt}, and hysteresis {Vh}. The resistance between nodes *A* and *B* transitions as the voltage at node *Ch_On* varies from $Vt - |Vh|$ to $Vt + |Vh|$. This transition is controlled by a polynomial function that is inherent to the operation of the switch model in LTspice [5].

The control signal for **S_Ch** is generated at node *Ch_On*. The voltage at node *Ch_On* is generated by the

circuit consisting of source **B_Ch_On**, resistor **R1** and capacitor **C1**. Source **B_Ch_On** implements a simple logical OR of the voltages at nodes *Delay_Over* and *Maintain*. LTspice uses a value of 0.5V as the threshold for logical operations. Thus, if the voltage at either node is greater than 0.5V, the output of **B_Ch_On** is 1V, otherwise it is zero. The addition of **R1** and **C1** provides for a finite rise time of the voltage at node *Ch_On* thus leading to a finite transition time for switch **S_Ch**. This time can be made insignificant in comparison to the time scales of interest while still providing a transition that is less likely to lead to simulation errors.

2) Breakdown Delay

One of the two values used to determine the state of **B_Ch_On** and thus the state of the switch **S_Ch** is the voltage at node *Delay_Over*. This voltage is generated by the source **B_Dly_Ovr**. The voltage of this source is determined based on a comparison of the voltage at two additional nodes, *T_Over* and *Delay*, which represent the time that the gap voltage has exceeded the static breakdown voltage and the breakdown delay time respectively. Thus, when the time that the gap voltage has been higher than the static breakdown voltage exceeds the breakdown delay time, the output of **B_Dly_Ovr** becomes 1V and this in turn drives the output of **B_Ch_On** to 1V and the switch **S_Ch** transitions to the on state.

The overvoltage time, represented by the voltage at node *T_Over*, is generated by source **B_T_Ovr** as the difference between the current simulation time and the most recent time that the gap voltage exceeded the static breakdown voltage. This time is represented, in units of seconds, by the voltage at node *T_B*. This voltage is generated by a sample and hold circuit. The node *Time* is a voltage representing the current simulation time that is generated by the source **B_Time**. Capacitor **C2** is charged to the value of V(*Time*) under control of switch **S1**. This switch is controlled by the source **B_!Ovr** which has a voltage equal to the logical inverse of the voltage at node *Over*. The value of V(*Over*) is determined by the relative values of the current gap voltage V(*V_Gap*) and the static breakdown voltage V(*V_Break*) through the source **B_Ovr**. The expression for the voltage of **B_Ovr** is an if-then-else that employs a hyperbolic tangent function to smooth the transition from the off to on state in order to eliminate discontinuities that could prevent convergence of the simulation solution. When V(*Over*) exceeds 0.5V, the output of **B_!Ovr** transitions from 1V to 0V and switch **S1** turns off – freezing the voltage of **C2** and thus the voltage at node *T_B*. This voltage now represents the time at which the overvoltage event began. The value of **C2** is theoretically arbitrary, but smaller values of **C2** limit the size of the current spike that occurs when **S1** re-closes after an overvoltage and thus improve convergence.

For the purposes of this model, the breakdown delay time is considered to be the time between the point at which the gap voltage exceeds the static breakdown voltage and the point at which the channel forms and conduction begins (i.e. the closing of switch **S_Ch**). The delay time, in units of seconds, is represented by the voltage at node *Delay*. This voltage is generated by behavioral source **B_Dly**. The output definition of **B_Dly** is one of the areas of this model for which there is no universally accepted expression and thus it is an area that the user may find benefit in experimentation. The present implementation makes use of the empirical formulation of T.H. Martin [6]:

$$t(E,\rho)=\frac{98700\times\left(\frac{E}{\rho}\right)^{-3.44}}{\rho}\ \text{(s)} \tag{1}$$

Where E is the average electric field in kV/cm and ρ is the gas volume density in g/cm^3. The electric field is calculated by the behavioral source **B_E_Gap** as the ratio of the current gap voltage to the user-input gap separation parameter {D} and is represented as the voltage at node *E_Gap* in units of V/m. The gas volume density is calculated by source **B_Rho** from the ideal gas law using the user input pressure parameter {P} and the STP density of air. The density is represented as the voltage at node *Rho_V* in units of kg/m^3.

While the present implementation of the breakdown delay is deterministic in nature and does not include the random component of the statistical delay, it should be possible to implement a physically realistic statistical delay using the random number functions available in LTspice if that behavior is important for a particular user.

3) Static Breakdown Voltage

The static breakdown voltage of the gap is represented in the model as the voltage at node *V_Break*. This voltage is generated by the source **B_V_Brk**. The expression for determining the value of static breakdown voltage is another area in which the user my find it useful to experiment with the various formulations that can be found in the large volume of literature pertaining to gas breakdown. Two different empirical formulations are available in the current implementation. For uniform field gaps filled with air at pressures of up to about 10 atmospheres, the formula presented by Meek and Craggs [7] is applicable:

$$V=24.55\left(\frac{P}{P_0}\right)d+6.66\left(\frac{P}{P_0}\right)^{\frac{1}{2}}d^{\frac{1}{2}}\ \text{(kV)} \tag{2}$$

Where P is the air pressure in the gap, P_0 is standard atmospheric pressure (760 Torr), and d is the gap distance in centimeters.

For very small gaps at high pressures, the formulation of Skilling and Brenner [8] is applicable:

$$V=\frac{30\left(\frac{P}{P_0}\right)d}{1+0.009\left(\frac{P}{P_0}\right)}+1.7\ \text{(kV)} \tag{3}$$

4) Channel Maintaining Current

After the initial closure of switch **S_Ch** resulting from the action of the breakdown delay circuitry described in the previous section, the voltage across the spark gap will rapidly collapse and current will begin to flow through the components **B_Ind**, **S_Ch**, and **B_Res**. In a physical spark gap, this current maintains a conductive channel through various physical processes. In the present model, an assumption has been made that there is some minimum value of this current that is required to maintain the channel in a conductive state. The value of this minimum current is represented by the voltage at node *I_Min* in units of A. The source **B_Maint** compares the magnitude of the channel current, represented by the voltage at node *I_Ch* with this minimum and generates a voltage of 1V when V(*I_Ch*) is greater than V(*I_Min*), otherwise the output is zero.

E. Channel Dynamics

The dynamic processes that occur after the initial breakdown of the spark gap are often of importance in the application of spark gaps and thus are important in the simulation of spark gaps. The present model seeks to provide a means of simulating these processes in a way that is easy to understand and can be easily tailored by the user to the particular requirements of a problem of interest. The dynamic elements that are modeled are the spark channel resistance and inductance. Figure 3 illustrates the circuitry used to control the simulation of these dynamic components.

1) Channel Resistance

The resistance of the spark channel after breakdown is modeled in the main circuit by voltage source **B_Res**. This source produces a voltage equal to the product of the current through itself and the voltage at node *R_Ch*, which represents the channel resistance in units of Ohms. The voltage at node *R_Ch* is generated by source **B_R_Ch**. Many expressions for the resistance of a spark channel as a function of various parameters have been presented in the literature. A useful overview is provided by Engel et.al. [9]. The present implementation of the model includes three such expressions – those of Vlastos [10], Toepler [11], and Kushner [12] – as user defined functions which may be substituted into the expression for the output of **B_R_Ch**. The proportionality constants for each of these expressions are those proposed by Engel. The expression for **B_R_Ch** also includes a limit function to provide lower and upper bounds on the channel resistance. These limits serve both to represent physical limits as well as to reduce the chances of simulation failure. The upper limit sets the maximum channel resistance that would be measured at the moment that an ionized channel has been established across the gap.

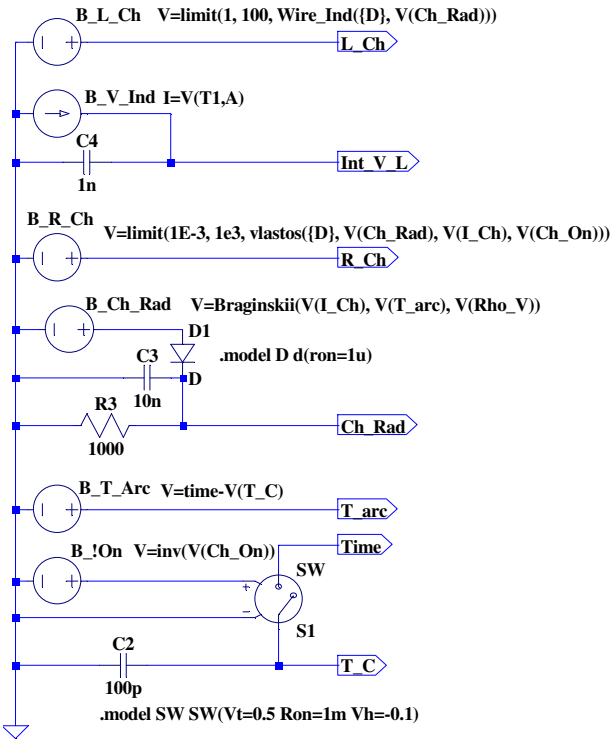

Figure 3. Channel Dynamics Control Circuitry

Some of these expressions make use of the channel radius as a parameter. Thus, a means has been provided in the present model to calculate the channel radius based on the well-known expression developed by Braginskii [13]:

$$\text{Radius} = 9.3\times10^{-4}\left(\frac{i^{\frac{1}{3}}\times t^{\frac{1}{2}}}{\rho^{\frac{1}{6}}}\right)\ (\text{m}) \qquad (4)$$

Where i is the channel current in kilo-Amperes, t is the time since the arc formed in microseconds, and ρ is the gas density in grams per cubic centimeter. This expression is used by source **B_Ch_Rad** to drive the voltage at node *Ch_Rad*, which then represents the arc channel radius in meters. The circuit consisting of **D1**, **C4**, and **R3** has been included because Braginskii's formulation was derived only to account for the shock-driven growth of the channel, not any contraction. Thus, **D1** allows **C4** to charge up to the peak output of **B_Ch_Rad** but then the voltage must decay via **R3**. The values of **R3** and **C4** should be chosen to give a time constant relatively long compared to the discharge event.

The Braginskii channel radius expression, as well as some of the arc resistance expressions found in the literature, require the time since arc formation as an input variable. Thus, a circuit to calculate the time since the last transition of the switch **S_Ch** from off to on has been incorporated into the model. This time is represented by the voltage at node *T_Arc* and is generated in the same way as the overvoltage time described above using the

logical inverse of the voltage at node *Ch_On* as the control signal for the sample and hold circuit that determines the arc start time at node *T_C*.

2) Channel Inductance

The inductance of the spark channel after breakdown is modeled in the main circuit by current source **B_Ind**. This source simulates an inductance by the method described by Basso in [14]. This method makes use of the fact that the governing differential equation of an inductor can be solved for the inductor current by separation of variables to give:

$$i(t)=\frac{\int_0^t v(\tau)d\tau}{L} \quad (5)$$

This formulation avoids the use of a time-derivative term, which will often produce significant errors in simulations. The voltage across the inductance is converted to a current by source **B_V_Ind** and this current is integrated by capacitor **C5**. This produces a voltage at node *Int_V_L* which is the time integral of the inductor voltage in units of Volt-seconds x 10^9. The current produced by **B_Ind** is then set to be the voltage at *Int_V_L* divided by the voltage at node *L_Ch*, which is used to represent the channel inductance in units of nano-Henrys. The voltage at node *L_Ch* is generated by the source **B_L_Ch**. The output of this source may be defined as a constant or as some expression of the other parameters in the model. In the present implementation, the expression for the inductance of an isolated thin wire derived by Grover [15] is used:

$$L=2d\left(\ln\frac{2d}{r}-0.75\right)\ (nH) \quad (6)$$

Where d is the gap distance in centimeters derived from the user input distance parameter {D} and r is the channel radius as determined by the voltage at node *Ch_Rad*. The expression used to calculate the voltage of **B_L_Ch** incorporates limits in order to bound the calculation. The inductance must not be allowed to reach zero, as that would drive the source **B_Ind** to infinite output. The upper limit keeps the output of **B_L_Ch** finite for very small values of channel radius. Thus, when the gap breaks down in the simulation and the channel radius begins to increase from zero, the rate of change of the output of **B_L_Ch** is limited. This reduces the chance of simulation errors.

III. USING THE MODEL

A. Challenges of Simulating Pulsed Power Circuits

As the primary goal of this work is to provide practitioners in the field of pulsed power with a spark gap model that can be used in the simulation of pulsed power circuits, it is necessary to point out some of the challenges that are inherent in the use of SPICE programs for such simulations. Most difficulties arise due to the very large rates of change of voltages and currents within a pulsed power system. Since LTspice, like all SPICE programs, was primarily developed for the simulation and design of relatively low voltage and power systems, the convergence tolerances have been set to values that are consistent with those applications. These tolerances are often too small to permit convergence of the solution of a pulsed power circuit. Fortunately, LTspice, and most other SPICE applications allow the user to change these tolerances to more suitable values. A second issue that often arises in the simulation of pulsed power systems is the fact that the impedances in these circuits are often highly reactive – which further exacerbates the issue of very high rates of change of currents and voltages. Furthermore, if one includes the various stray reactances that are common in such circuits in the model, numerous resonances will exist and can quickly overtax the simulation. This issue is compounded further by the perfect nature of the reactive components provided in SPICE software. Without the addition of suitable lossy elements (i.e. parasitic resistances) the oscillations of these resonances will be undamped and thus may grow without bound – leading to simulation failure.

B. Techniques to Prevent Simulation Failure

Successful simulations of pulsed power systems, like all simulations, require that the experimenter be sufficiently familiar with the physics of the problem as well as the limitations of the simulation tool. This will enable one to quickly determine if the results of a simulation are unreasonable and thus take action to refine the model for more accurate results. In the case of simulating common pulsed power circuits, several techniques have been found to be helpful in obtaining useful results when using the present model. These techniques are discussed in the following sections in order of descending desirability.

1) Addition of Parasitic Elements

First, it is important to include realistic values for the lossy parasitics of the circuit under consideration. This includes capacitor and inductor series resistances. The addition of a large value shunt resistance on inductors can improve the simulation circuits where the inductance dominates the load impedance.

2) Changes in Circuit Values

It has been observed that in some cases, simulation failures occur due to the interaction of the values of various circuit components. In these cases, small changes in the values of circuit components, on the order of 1% or less, have resulted in successful simulation convergence. Since the actual resistances, inductances, etc of a pulsed power circuit are rarely known to better than 1%, this technique can often be applied with no real impact on the accuracy of the results.

3) Alternative Simulation Settings

LTspice and most other SPICE programs allow the user to choose between certain settings of the simulation algorithm. In particular, most SPICE software includes various alternatives for the numerical integration technique used to transform the circuit differential equations into algebraic equations. In some cases, a simulation that fails with the default method, will successfully run with an alternative technique. Often, the main sacrifice is in the speed of the simulation. LTspice includes an additional selection of an alternative matrix solver, which can improve simulation convergence by reducing internal rounding errors with some penalty in simulation speed [5].

4) Changing Simulation Tolerances

The final technique that may be used to get a simulation to run successfully is to relax some of the tolerances used by the software. This should only be done when the previously mentioned techniques have failed to yield results and changes should be made in a gradual and methodical manner.

There are four primary tolerances in all SPICE-based simulation software that may be useful in improving simulation convergence. The first is the relative tolerance – denoted RELTOL. This parameter, which generally defaults to 0.001, defines the tolerance for the estimated error of any given node voltage or branch current relative to the present value at each time step of the simulation. This can be thought of as a measure of the relative accuracy of the solution at each point. The next two tolerances are the absolute current tolerance – denoted ABSTOL – and the voltage tolerance – denoted VOLTOL. These provide lower limits for the tolerance of the branch currents and node voltages. These are particularly important near zero-crossings where the relative tolerance approaches zero. These first three tolerances work together to determine how much estimated error is permitted in the solution at each time step. In general, increasing these tolerances can allow a failing simulation to run – at the expense of reduced accuracy and the increased risk of the appearance of simulation artifacts. The fourth tolerance is the general transient tolerance – denoted TRTOL. This parameter affects the dynamic adjustment of the simulation time step size with larger values permitting more truncation error in the numerical integration before the time step is reduced. Increasing this tolerance will generally permit larger time steps and can allow the simulation to step past a point that is causing convergence problems. However, this can lead to poor results and simulation artifacts. Conversely, reducing this tolerance can sometimes improve simulation success by forcing the algorithm into smaller time steps that improve tracking of the circuit behavior near discontinuities.

C. Tailoring the Model

The present model has been developed with the intent of providing practitioners in the field of pulsed power engineering with a useful tool for the simulation of pulsed power circuits in commonly available circuit simulation software. Since many of the physical processes at work in a spark gap are still actively under investigation, this model has been built in such a way as to permit the easy incorporation of new models for the various physical processes as new information may become available. Once the user becomes familiar with the model, changes can be easily made by substituting the desired expression into the value parameter of the applicable behavioral source.

IV. REFERENCES

[1] J. G. Zola, "Gas Discharge Tube Modeling With PSpice," *Electromagnetic Compatibility, IEEE Transactions on*, vol. 50, no. 4. pp. 1022–1025, 00-2008.

[2] B. Martin, P. Raymond, and J. Wey, "New model for ultracompact coaxial Marx pulse generator simulations," *Rev. Sci. Instruments*, vol. 77, 2006.

[3] C. Basso, "Spark Gap Modeling," *Intusoft Newsletter*, no. 50, pp. 9–13, Sep-1997.

[4] M. Narui and F. P. Dawson, "A SPICE model for simulating arc discharge loads," 1991.

[5] M. Engelhardt, "LTspice IV Help File." Linear Technology Corporation, Dec-2014.

[6] T. H. Martin, "An empirical formula for gas switch breakdown delay," in *Pulsed Power Conference, 1989. 7th*, 1989, pp. 73–79.

[7] J. M. Meek and J. D. Craggs, *Electrical Breakdown of Gases*. Wiley, 1978.

[8] H. H. Skilling and W. C. Brenner, "The electric strength of air at high pressure - II," *Trans. Am. Inst. Electr. Eng.*, vol. 60, no. 3, Mar. 1941.

[9] T. G. Engel, M. Kristiansen, and A. L. Donaldson, "The pulsed discharge arc resistance and its functional behavior," *IEEE Trans. Plasma Sci.*, vol. 17, pp. 323–329, Apr. 1989.

[10] A. E. Vlastos, "The Resistance of Sparks," *J. Appl. Phys.*, vol. 43, p. 1987, 1972.

[11] M. Toepler, "Zur Kenntnis der Gesetze der Gleitfunkenbildung," *Ann. Phys.*, vol. 21, no. 2, pp. 193–222, 1906.

[12] M. J. Kushner, W. D. Kimura, and S. R. Byron, "Arc resistance of laser triggered spark gaps," *J. Appl. Phys.*, vol. 58, pp. 1744–1751, Sep. 1985.

[13] S. I. Braginskii, "Theory of the Development of a Spark Channel," *J. Exp. Theor. Phys.*, vol. 34, pp. 1068–1074, Dec. 1958.

[14] C. Basso, "SPICE analog behavioral modeling of variable passives," *Power Electronics*, p. 57, Apr-2005.

[15] F. W. Grover, *Inductance Calculations*. Mineola, USA: Dover Publications Inc, 2009.